Naunyn-Schmiedeberg's Archives of Pharmacology (2023) 396:99–108
https://doi.org/10.1007/s00210-022-02299-z

RESEARCH

Norcantharidin toxicity profile: an in vivo murine study

Gabriel Martínez-Razo[1] · María Lilia Domínguez-López[2] · José M. de la Rosa[3] · Diego A. Fabila-Bustos[4] · Elba Reyes-Maldonado[5] · Eliezer Conde-Vázquez[6] · Armando Vega-López[1]

Received: 17 June 2022 / Accepted: 22 September 2022 / Published online: 3 October 2022

Abstract

Norcantharidin (NCTD) is the demethylated analog of cantharidin, with allegedly reduced toxicity. However, there is still limited information regarding its posology and potential risk in its use in cancer treatment. Healthy BDF1 mice were intraperitoneally administered with norcantharidin (0, 3, 6, 12, and 25 mg/kg) every 24 h for 6 days. Survivor mice were euthanized, and the brain, lungs, kidneys, spleen, and liver were procured for enzymatic and histopathological analysis in the liver and kidney. DL_{50} were 8.86 mg/kg for females and 11.77 mg/kg for males. The treatments with 3.0 mg/kg and 6.0 mg/kg significantly modified the phosphorylase, alanine transaminase, and γ-glutamyl transferase activities; however, an organ-specific response was detected. A significant dose-dependent decrease was observed in the kidney for ROS, while the liver had the opposite effect. Histopathological analysis revealed a significant elevation in hepatocytes' nuclei average size and total area (3 mg/kg), as well as centrilobular vein and adjacent sinusoidal capillaries showed a significant difference. The portal triad presented a significant difference in veins and capillarity count in 6 mg/kg. Renal samples showed cortex convoluted tubules' average size significantly augmented in both doses' groups, and tubule count was found augmented in 6 mg/kg. These physiological effects of NCTD can be exploited as treatment strategies if able to operate in an established posology and proper testing.

Keywords Norcantharidin · Toxicity · Phosphatase · Safety dosage

Introduction

Meloidae family defensive agent, cantharidin (3a,7a-Dimethylhexahydro-4,7-epoxyisobenzofuran-1,3-dione; formula: $C_{10}H_{12}O_4$; CAS-No. 56–25-7) produce by the beetles for fertilized egg protection, is a terpenoid compound widely used in traditional eastern medicine. Although misused in several applications, such as an aphrodisiac, western dermatology practice employed it as a topical treatment for furuncles, piles, warts, and molluscum contagiosum. While it is relatively safe when used as a colloidal solution in 0.7–0.9% of cantharidin should be restricted to a dermatologist's office or under direct supervision (Moed et al. 2001). Application of cantharidin in the skin causes the release of neutral serine proteases, triggering desmosome plaque degradation and, subsequently, detachment of tonofilaments

✉ Armando Vega-López
avegalo@ipn.mx; avegadv@yahoo.com.mx

1 Instituto Politécnico Nacional, Escuela Nacional de Ciencias Biológicas, Laboratorio de Toxicología Ambiental, Unidad Profesional Zacatenco, Av. Wilfrido Massieu s/n, CP 07738 Mexico City, Mexico

2 Instituto Politécnico Nacional, Escuela Nacional de Ciencias Biológicas, Laboratorio de Inmunoquímica I, Casco de Santo Tomás, Carpio y Plan de Ayala S/N, Mexico City, CP 11340, México

3 Instituto Politécnico Nacional, Escuela Superior de Ingeniería Mecánica Y Eléctrica (ESIME) Unidad Zacatenco, Unidad Profesional Zacatenco, CP 07738 Mexico City, Mexico

4 Instituto Politécnico Nacional, Unidad Profesional Interdisciplinaria de Ingeniería, Campus Hidalgo (UPIIH), Carretera Pachuca - Actopan Kilómetro 1+500 Ciudad del Conocimiento y la Cultura Educación, 42162 Hidalgo, México

5 Instituto Politécnico Nacional, Escuela Nacional de Ciencias Biológicas, Laboratorio de Hemopatología, Carpio y Plan de Ayala S/N, Casco de Santo Tomás, Mexico City CP 11340, México

6 Hospital Bicentenario de La Independencia del Instituto de Salud de Trabajadores del Estado ISSSTE, Ciruelos 4, Lázaro Cárdenas, Tultitlán de Mariano Escobedo, Tultitlan Estado de México CP 54916, México

from desmosomes. Intraepidermal blistering, acantholysis, and unspecific lysis of the epidermis are a consequence of cantharidin-induced lesions. The dermatologist monitors and controls the area and intensity of blistering by washing the affected area with soap and water,blisters heal after 4 to 7 days without scarring (Dorn et al. 2009).

Complications and poisoning of cantharidin are caused more often by accidental beetle ingestion. Among the adverse effects or complications are erythema, pruritus, and severe blistering in skin and mucosa. Clinical signs and symptoms are not specific, although burning sensation in the digestive tract, dysphagia, hematemesis, and vomiting are frequent. Also, after prolonged exposure, it has been reported to cause pseudo-polycythemia and even neurological complications such as a Guillain Barré-like syndrome (Harrisberg et al. 1984). Damage is dose-dependent, with a fatal dose estimated in the wide range from 10 to 65 mg/kg and the median lethal dose at 1 mg/kg (Neumann et al. 1995). Casualties result from renal failure after dysuria, proteinuria, and hematuria (Linck et al. 1996). Although cantharidin is too toxic to be administered systemically, it is possible that safer derivatives, such as norcantharidin, offer new potential therapeutic options for several applications (Honkanen 1993).

Norcantharidin (7-oxabicyclo heptane-2,3-dicarboxylic acid; formula: $C_8H_8O_4$; CAS-No. 29745–04-8; NCTD) is the demethylated analog of cantharidin, easier to synthesize and allegedly reduced toxicity (Xie et al. 2019). Both cantharidin and norcantharidin (Fig. 1) had shown to inhibit protein phosphatases PP1 and PP2, which play a vital role in the regulation of the cell cycle (Dorn et al. 2009). Also, its anhydride moiety has been proposed to be the active site that triggers its antitumoral function tested in treating various types of cancer, like neuroblastoma and glioblastoma (Pachuta-Stec and Szuster-Ciesielska 2015). Recent and well-conducted review detailed specific information about the role of NCTD in the treatment of different cancer (Zhou et al. 2020). However, there is still limited information regarding its toxicity, side effects, posology, and potential risk in its use. This study aims to provide information in a murine model that might fill gaps concerning this matter, establish a safe dose, and determine its effect at a systemic level, biochemically and morphologically.

Materials and methods

Experimental design

The study protocol was approved by the local Ethical Committee (license number: PE/001/2574–6/20). The study was divided into two phases: the exposure phase and the post-euthanized biochemical and histopathological image analysis.

Mice and acclimatization

Healthy BDF1 mice ($n=65$) of 9–13 weeks of age, both sex, with an average body weight of 30 g were obtained from the National School of Biological Sciences, Mexico. Mice were maintained in the bioterium under 12:12-h dark: light cycle at 23 °C and 40–60% humidity, with water and food provided ad libitum, in agreement with Article 38 and Chapter V of the Directive 2010/63/EU of the European Parliament and of the Council of 22 September 2010 on the protection of animals used for scientific purposes.

Exposure treatments

Mice were randomly distributed in five groups ($n=13$): Control group, 3 mg per body weight in kilograms (mg/kg), 6 mg/kg, 12 mg/kg, and 25 mg/kg in 100 µL of volume. Each experimental group was administered with norcantharidin (CAS Number: 29745–04-8; Merck, USA) intraperitoneally

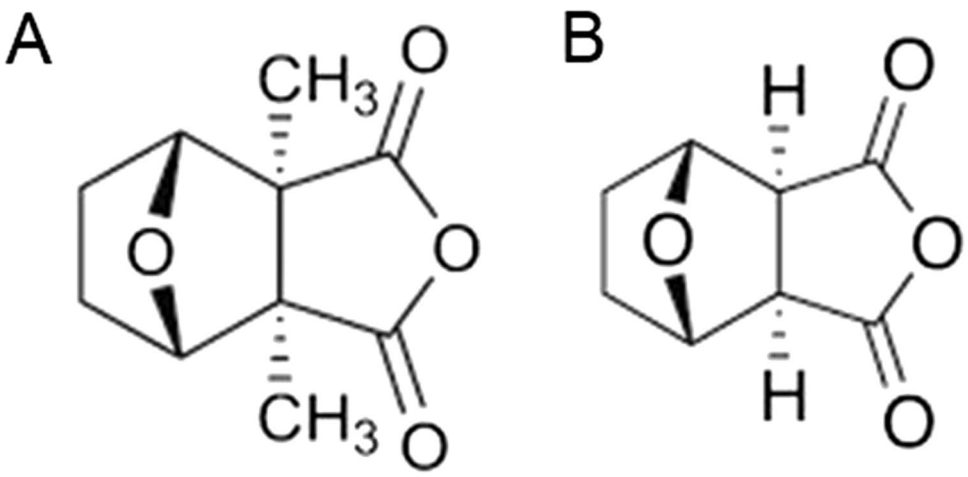

Fig. 1 Chemical structures of cantharidin (**A**) and its demethylated analog Norcantharidin (**B**)

every 24 h for 6 days (144 h). The median lethal dose (LD_{50}) was calculated by sex to determine the acute toxicant activity of norcantharidin. Also, a survival probability analysis was calculated for each group.

Survivor mice were further included into the subsequent analysis regardless genre, to provide robustness into the data. Mice were sedated with a 4% isoflurane anesthesic vaporized chamber (RWD™) with a 0.5-L/min flux and euthanized with cervical dislocation by the end of the exposure. The brain, lungs, kidneys, spleen, and liver were procured and divided into two different tissue conservation procedures: one part was kept in a pre-weight microfuge tube with 1.0 mL of PBS buffer solution (1.0%, pH ~ 7.4); and the other part in a 50-mL Falcon tube with 10 mL of 10% buffered neutral formalin as a fixing agent for later processing.

Serum panel

Blood samples were obtained by cardiac puncture and pooled in tubes with sodium citrate (109 mmol/L) as anticoagulant. Tissues preserved in PBS buffer solution were macerated and centrifuged at 9000 × *g* for 15 min at 4 °C. Serum clinical chemistry tests were performed by biochemistry analyzer (Thermo Fisher) with commercially available kits (Spinreact) using photometric and colorimetric testing adjusted for rodents.

Enzymatic activity

Samples of S9 fractions were adjusted by the amount of tissue and presented as mol per gram of tissue. To evaluate lactate dehydrogenase (LDH; EC 1.1.1.27), volumes of 200 µL of S9 fraction were added to 800 µL of buffer pH 7.0 of Imidazole 65 mmol/L and pyruvate 0.6 mmol/L, and measured photometrically at 340 nm. For alanine aminotransferase (EC 2.6.1.2), 800µL buffer of TRIS pH 7.8 enriched with 1200 U/L of LDH and 500 mmol/L of L-Alanine were added to samples and measured at a 340 nm. As for the gamma-glutamyl transferase (γGT; EC 2.3.2.2), samples were added to 800 µL of TRIS buffer pH 8.6 and 100 mmol/L of glycylglycine. and measured at 405 nm. Protein phosphatase-1 (EC 3.1.3.16) as described in Nájera-Martínez (Nájera-Martínez et al. 2022). Enzymatic activities were calculated by molar extinction coefficient. All samples were evaluated using a Synergy MX spectrofluorometer (BioTek).

Antioxidant activity and ROS levels

The superoxide dismutase (EC 1.15.1.1) evaluation method of Misra and Fridovich (Misra and Fridovich 1972) evaluates the inhibition rate of epinephrine autoxidation, measured by absorbance at 480 nm as a sensitive assay for this enzyme. The reactive oxygen species (ROS) was evaluated by the specific oxidation of dihydroethidium, and dihydrofluorescein diacetate at 480 nm (Dzul-Caamal et al. 2016) in the Synergy MX spectrofluorometer (BioTek).

Histopathological analysis

Liver and renal samples were processed with the paraffin inclusion technique and stained with hematoxylin and eosin. Liver micrographs of 3 microns thick slices (Microtome RM2245, Leica microsystems) were obtained at the centrilobular vein ($n = 9$) and the portal triads ($n = 9$) at 20 × augmentation. Renal pieces were sliced at the cortex region ($n = 9$) and micrographs were obtained at 40 × augments using an optical microscopy (Binocular optical microscope Leica microsystems) (Madera-Sandoval et al. 2019).

Image analysis

An object- and spatial-level quantitative analysis of multispectral histopathology images was performed using Image J software (NIH, Bethesda, MA, USA, available in: https://imagej.nih.gov/ij/) (Schneider et al. 2012). Micrographs were transformed from 32-bit into 8-bit images for nuclei analysis and filtered by erode mode (element: disk,size: 1 pixel of diameter) using the morphological filter plugin MorphoLibJ (Legland et al. 2016). Afterward, a max entropy threshold selection was performed, which contrasts the area of hematoxylin pigment. Furthermore, 8-bit micrographs were processed to analyze the veins and adjacent sinusoidal capillaries at the centrilobular region and the portal triads region of liver samples, and renal samples cortex region convoluted tubules and corpuscles. Consequently, micrographs were filtered by opening mode (element: disk,size: 2 pixels of diameter), and an image threshold selection was performed using Otsu's threshold to contrast empty gaps of the micrographs. Micrographs' selected regions were measured through the particle analysis feature, which provides particle count, total area, and average size by pixel transformation.

Data analysis

Norcantharidin exposure survival rate data were analyzed with probit-log regression model with 95% fiducial limits, and comparisons of these fits were made using differences in deviance as a chi-square ($\chi 2$). Furthermore, a Kaplan Meier survival analysis was performed using R for Statistical Computing (R Core Team 2022). Median lethal dose (LD_{50}) was calculated using standard errors and covariances of slopes and intercepts of probit fits (Wald test). Enzymatic fluorescence and absorbance assays were statistically described for symmetric distribution fitness with Anderson Darling and compared with ANOVA when data showed the goodness of fit with Dunnett's post hoc comparison test or

Kruskal–Wallis if data showed non-normal behavior. Statistical comparisons were calculated using PAST version 2.17c. (Hammer et al. 2001), and plots (figures) were made with Sigma Plot (Version 11.0 Buil 11.0.0.77, Systat Software, Inc., 2008).

Results

Treatments survivors' mice showed ill resemblance and lack of strength before euthanizing. A macroscopic evaluation revealed damage in internal organs such as hepatomegaly, splenomegaly, and bladder obstruction (results not showed). Lethal dose 50 (LD_{50}) values calculated for NCTD at 48 h were 8.86 mg/kg for females ($p \leq 0$ 0.01) and 11.77 mg/kg for males ($p \leq 0$ 0.01). In addition, lethal dose 10 and 1 (LD_{10} and LD_1) were calculated for females at 5.71 and 3.99 mg/kg and for males 8.44 and 6.47 mg/kg, respectively. The Kaplan–Meier survival analysis was performed to calculate survival probability to a 144-h norcantharidin exposure at of 0.92 for 6 mg/kg, 0.39 for 12 mg/kg, and 0.08 for 25 mg/kg (Fig. 2; $p < 0.0001$, C.I.95%).

Serum glucose values were found reduced in both treatments, compared to the control group. In both treatments, urea values showed an upward tendence, but no significance was found. Creatinine was found augmented half as much in the 3 mg/kg treatment and altered in the 6 mg/kg but with no significance. In general, proteins in blood were altered which highly suggest liver and kidney stress. Notably, the ratio albumin/globulin was significantly low in the 3 mg/kg treatment but again, non-significant in the 6 mg/kg treatment. Mild disturbances in electrolytes levels were found although none of them reach significance (Table 1).

Phosphorylase activity was significantly augmented in all tissues in the 6 mg/kg dose, except for the kidney. For the 3 mg/kg dose, a significant activity rise was found in the brain and liver compared to the control group. Compared to the control group, a significant elevation of alanine transaminase activity was found in the kidney in the 6 mg/kg dose group, and so for the lung and liver in the 3 mg/kg dose.

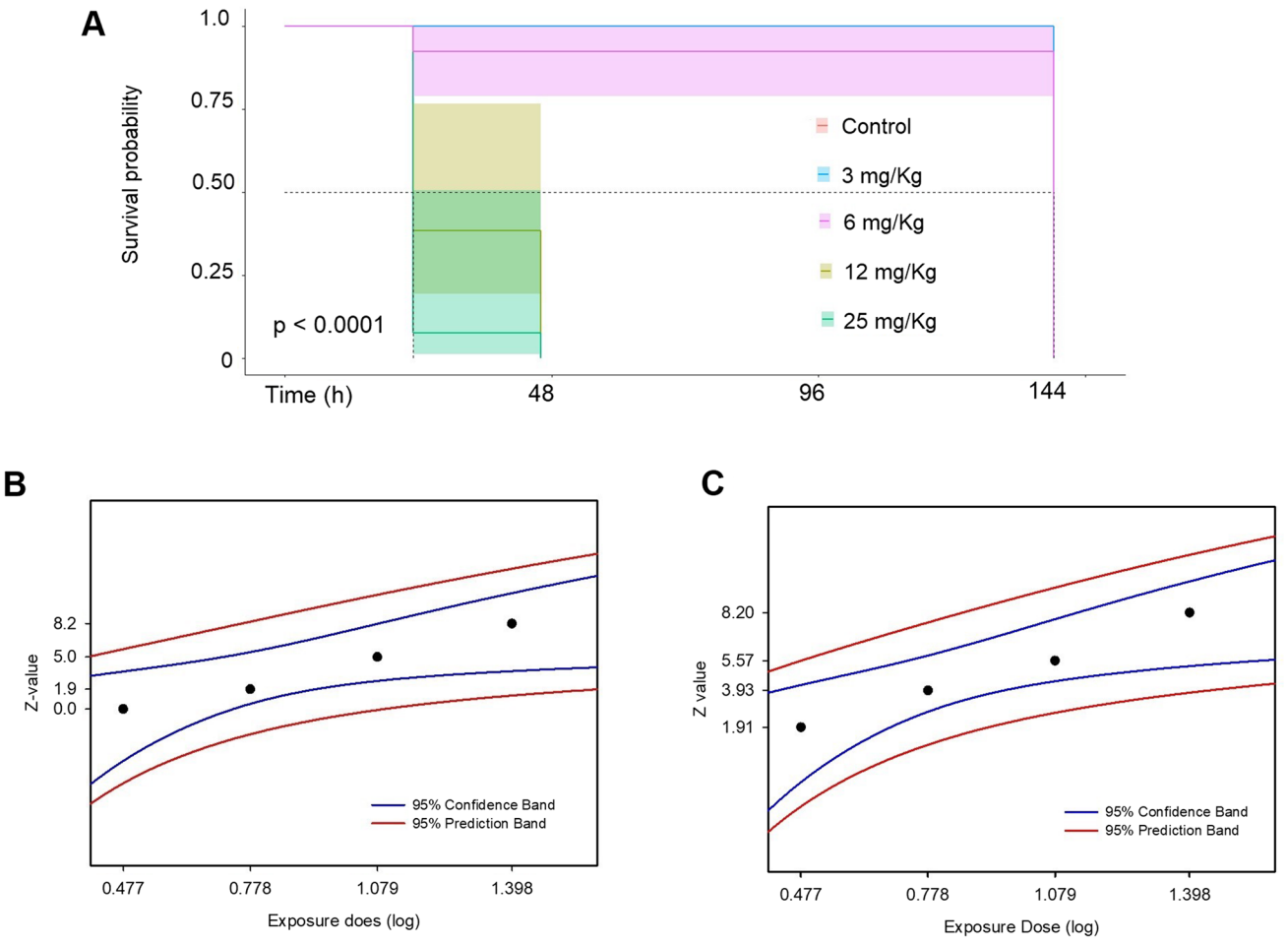

Fig. 2 **A** Survival plot for mice exposed to different doses of norcantharidin; and probability graphical representation of the estimated probit regression equation with 95% confident intervals, and prediction band. **B** Male mice. **C** Female mice

Table 1 Serum metabolic panel at different exposure schemes of norcantharidin

Analyte	Units	Control		3 mg /Kg			6 mg/ Kg		
Cholesterol	mmol/L	2.85	1.02	5.15	1.53	*	4.39	0.8	N.S
Total proteins	g/L	88.25	44.5	196	67.7	*	161.25	35.4	N.S
Albumin (A)	g/L	39.5	14.6	69.25	19.3	*	61.5	9.7	N.S
Creatinine (C)	µmol/L	30.25	2.62	45.25	9.06	**	39	4.69	N.S
Globulin (G)	g/L	48.7	30.1	126.7	48.6	*	93	36.4	N.S
A/G	ratio	0.93	0.29	0.57	0.08	*	0.69	0.08	N.S
Urea nitrogen	mmol/L	8.45	0.86	8.57	0.75	N.S	9.6	0.94	N.S

Means ± standard error. *N.S* no significance; * $p \leq 0{,}05$; ** $p \leq 0{,}01$ statistically significant

As for the γ-glutamyl transferase, both doses significantly increased enzyme activity compared to the control group, except for the lung (Table 2). For reactive oxygen species (ROS), a significant dose-dependent decrease was observed in the kidney, while the liver had the opposite effect. In comparison, the superoxide test showed a steady increase for the spleen and an increase in the kidney and liver to 3 mg/kg, and then a depletion to 6 mg/kg (Fig. 3).

Hepatocytes were found polygonal with rarefactional changes of cytoplasm and a frequency of 3 to 4 per high magnification field. Cords were arranged into one-cell-thick threads, and sinusoidal gaps diminished. Centrilobular veins showed discreet vascular congestion, and portal triads with visible bile ducts in treated samples. Glomeruli was found to be uniform in size distribution with an average cellularity of 4 to 5 cells per mesangial region with visible basal membrane, and patent capillary. Cortex convoluted tubules and corpuscles were preserved with tall cubic-columnar cells, forming a vast cladding layer structure, eosinophilic cytoplasm, round, and conspicuous nucleolus, while medullary tubules were cubic, short and had a packed appearance (Fig. 4, images).

Image analysis revealed a significant elevation in hepatocytes' nuclei total area and average size in the 3 mg/kg group. The centrilobular vein and adjacent sinusoidal capillaries showed a significant difference in their count, total area, and average size in the 6 mg/kg dose. The portal triad showed only a significant difference in veins and capillarity

Table 2 Biochemical testing in different tissues, with different exposure schemes of norcantharidin

Enzyme	*Tissue*	Control		3 mg /Kg			6 mg/ Kg		
		Mean	±*S.E*	Mean	±*S.E*	*sig*	Mean	±*S.E*	*sig*
Phosphorylase	*Brain*	$0.51E^{-05}$	$0.9E^{-06}$	$1.11E^{-05}$	$1.5E^{-06}$	**	$0.94E^{-05}$	$0.9E^{-06}$	**
	Lung	$2.38E^{-05}$	$4.3E^{-06}$	$4.03E^{-05}$	$6.4E^{-06}$		$5.43E^{-05}$	$5.3E^{-06}$	**
	Kidney	$7.49E^{-05}$	$0.2E^{-06}$	$11.0E^{-05}$	$8.4E^{-06}$		$4.74E^{-05}$	$3.0E^{-06}$	
	Spleen	$3.32E^{-05}$	$0.1E^{-06}$	$4.31E^{-05}$	$4.4E^{-06}$		$6.23E^{-05}$	$9.9E^{-06}$	*
	Liver	$1.00E^{-05}$	$2.1E^{-06}$	$2.01E^{-05}$	$2.6E^{-06}$	*	$2.12E^{-05}$	$3.2E^{-06}$	*
Lactate dehydrogenase	*Brain*	$2.53E^{-01}$	$4.8E^{-02}$	$2.33E^{-01}$	$3.1E^{-02}$		$2.68E^{-01}$	$3.5E^{-02}$	
	Lung	$8.02E^{-01}$	$0.1E^{-02}$	$6.79E^{-01}$	$8.9E^{-02}$		$4.57E^{-01}$	$0.1E^{-02}$	
	Kidney	$5.27E^{-01}$	$0.1E^{-02}$	$4.16\ E^{-01}$	$5.6E^{-02}$		$2.96E^{-01}$	$4.4E^{-02}$	
	Spleen	$7.14E^{-01}$	$0.1E^{-02}$	$8.77E^{-01}$	$0.1E^{-02}$		$6.94E^{-01}$	$8.5E^{-02}$	
	Liver	$1.83E^{-01}$	$2.7E^{-02}$	$2.07E^{-01}$	$3.7E^{-02}$		$2.14E^{-01}$	$2.2E^{-02}$	
Alanine transaminase	*Brain*	$3.86E^{+02}$	$0.3E^{+01}$	$3.97E^{+02}$	$0.8E^{+01}$		$3.97E^{+02}$	$1.0E^{+01}$	
	Lung	$4.08E^{+02}$	$0.5\ E^{+01}$	$4.41E^{+02}$	$1.2E^{+01}$	*	$4.32E^{+02}$	$0.6E^{+01}$	
	Kidney	$4.18E^{+02}$	$0.8\ E^{+01}$	$4.24\ E^{+02}$	$0.8E^{+01}$		$4.45E^{+02}$	$1.0E^{+01}$	
	Spleen	$4.15E^{+02}$	$0.6\ E^{+01}$	$4.2\ E^{+02}$	$1.3E^{+01}$		$4.60E^{+02}$	$1.3E^{+01}$	*
	Liver	$4.51E^{+02}$	$0.1\ E^{+01}$	$5.97E^{+02}$	$5.7E^{+01}$	*	$5.39E^{+02}$	$2.4E^{+01}$	
Gamma glutamyl transferase	*Brain*	$1.27E^{+02}$	$0.5\ E^{+01}$	$1.35E^{+02}$	$0.3\ E^{+01}$	*	$2.07E^{+02}$	$3.5E^{+01}$	*
	Lung	$2.09E^{+02}$	$3.9E^{+01}$	$2.33E^{+02}$	$2.5E^{+01}$		$2.07E^{+02}$	$2.2E^{+01}$	
	Kidney	$2.83E^{+02}$	$5.4E^{+01}$	$5.81\ E^{-02}$	$7.4E^{+01}$	**	$4.14E^{+02}$	$4.6E^{+01}$	*
	Spleen	$1.53E^{+02}$	$1.2E^{+01}$	$1.91E^{+02}$	$2.1E^{+01}$	*	$2.51E^{+02}$	$3.7E^{+01}$	**
	Liver	$1.32E^{+02}$	$0.3\ E^{+01}$	$2.02E^{+02}$	$1.5E^{+01}$	**	$1.73E^{+02}$	$1.0E^{+01}$	**

Data showed as *mol per gram of tissue* means ± standard error. * $p \leq 0.05$; ** $p \leq 0.01$ significantly different compared to the control group

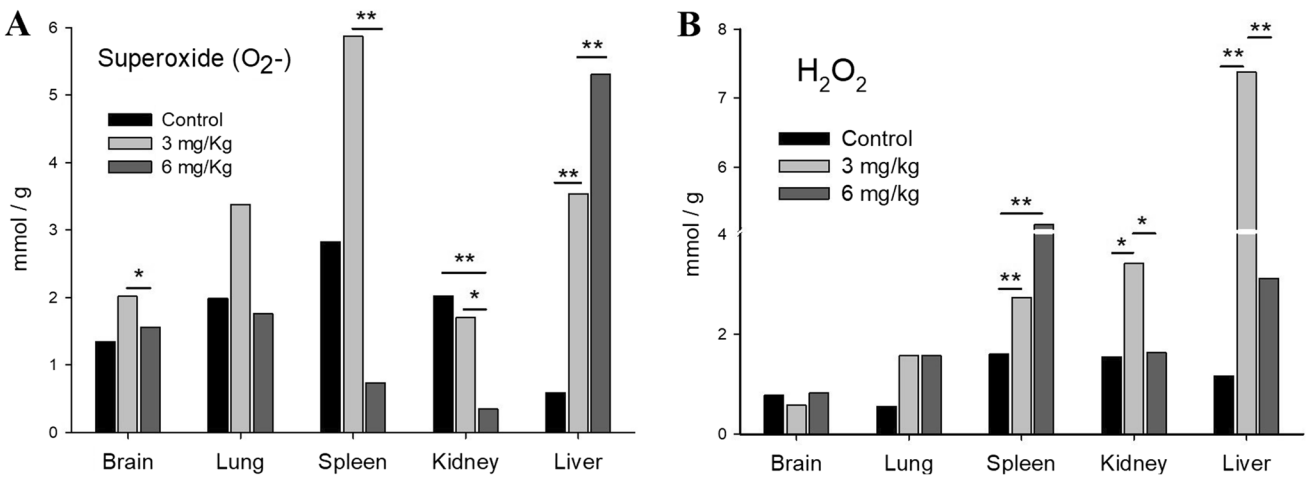

Fig. 3 Graphical representation of reactive oxygen species (ROS) content in all tissues exposed to different norcantharidin doses. **A** Superoxide ($O_2.^-$). **B** Hydrogen peroxide content.* $p < 0.05$; ** $p < 0.01$

count in the 6 mg/kg dose group. Renal samples showed cortex convoluted tubules' average size significantly augmented in both doses' groups, although tubules count was found augmented in the 6 mg/kg dose group (Fig. 4; graphics).

Discussion

Norcantharidin use in humans has not been well established as it is not approved by any regulatory entity nor included in the European or American pharmacopeias. Namely, there is no consensus on the best administration route for this molecule. Moreover, no clinical trial is currently available for any clinical application. To our knowledge, the closest approach to this matter is the administration of norcantharidin in eastern medicine, more specifically in Chinese traditional practice, to treat esophagus and stomachal cancer. Further, norcantharidin use is limited due to its low solubility, with a maximum solubility in water of 2.5 mg/ml at pH = 6, increasing to 9.5 mg/ml at pH = 9.5 (Lu et al. 2012). Usage of NCTD includes oral, intravenous administration, and local injection of its sodium salt, which causes intense irritation at the injection site (Pan et al. 2020).

Norcantharidin has been proposed for many pharmacological purposes, but mainly as a chemotherapeutic agent. However, there is limited information on the toxicological effects that NCTD exposure has in a non-pathological scenario. In our results, the highest dosage group (25 mg/kg) of female mice died in the first 48 h and all-male mice at 96 h. Moreover, in the 12 mg/kg dosage group, all animals perished at 144 h, except one male eliminated from further analysis. For the lower dosage groups, only one female mouse perished in the 6 mg/kg group the first 48 h, and in the 3 mg/kg dosage group and control group, no animal perished. LD_{50} was calculated at 8.86 mg/kg for females and 11.77 mg/kg for males. This contrasts with previous work; while Dorn (Dorn et al. 2009) reported a maximum tolerated dose of 2.5 mg/kg of body weight, Mei (Mei et al. 2019) used a 25 mg/kg dosage. However, the LD_{50} found in the current study is similar to that reported in mice intravenously treated with 10 mg/kg by the US Army Armament Research & Development Command, Chemical Systems Laboratory NIOSH Exchange Chemicals. Vol. NX#05,066 (https://chem.nlm.nih.gov/chemidplus/rn/5442-12-6).

Sex differences in susceptibility to toxic agents have never been completely delineated. It has been proposed that the underlying mechanism may be related to genetic differences in biological responses. Studies have included the effect of sex hormones administration, pregnancy, and the influence of castration. (Friedman et al. 1972). For example, the subfamily of cytochrome P450 4A (rodents: *cyp4a*,humans: CYP4A) catalyzes xenobiotics' oxidation and is predominantly expressed in the liver and kidney, as well as stands out the activity of aromatase. Mouse *cyp4a* have shown strain- and gender-specific expression patterns in these organs. Sex hormones and gender dimorphic growth hormone (GH) patterns may contribute to gender-specific differences in xenobiotic metabolism (Zhang and Klaassen 2013).

Serum metabolic panel revealed dysregulation of metabolic analytes that suggest mainly liver damage, and to a less extent, in renal tissue. Drugs frequently cause hypoglycemia by interfering with glucose metabolism. Glucose levels fall in serum might be consequence of allosteric glycogen synthesis upregulation due to liver phosphorylases inhibition. Also, cholesterol which plays an essential role in steatohepatitis pathogenesis is altered in norcantharidin treatments (Ben Salem et al. 2011). Cholesterol de novo synthesis is obtained from acetyl CoA by

hydroxymethylglutaryl-CoA synthase. Different studies revealed that the expression and activity of these enzymes are increased in patients with liver damage and are associated with a decrease in the levels of phosphorylation of its active form (Min et al. 2012). Moreover, although creatinine is formed in muscles from phosphocreatine, phosphorylated creatine is synthesized primarily in the liver and transported to the muscles as a storage depot for muscle energy. Creatinine levels may arise by augmented energy demand and phosphocreatine depletion by phosphorylation inhibition (Bjornsson 1979).

Hyperalbuminemia is common in serum volume contraction secondary to fluid losses. Globulins may also increase in this situation, resulting in hyperproteinemia with no change in A:G ratio. However, the low A:G ratio suggests liver and renal damage, as well as systemic inflammation. Prednisolone increased serum glucose concentration, and albumin concentrations by 15–17%, in a non-dose-dependent manner, in eight Beagle dogs given 0.5, 1.2, and 4 mg/kg/d for 5 days (Tinklenberg et al. 2020).

Enzyme tests revealed augmented activity in those related to NCTD binding activity sites, such as protein phosphatase-1 (Mei et al. 2019; Li and Casida 1992) and those related to hepatic function. Alanine transaminase elevated tissue activity is related to reversible drug-induced hepatic cell damage before clinical symptoms and signs (Vroon et al. 1990). However, interpretation of glutathione results is far more complicated because liver weight increases after bile duct ligation. Results vary according to whether glutathione content is related to tissue mass or total content per liver. Glutathione plays an essential role in protecting cells against oxidants produced during normal metabolism. If oxidative stress increases, then so will the requirement for reduced glutathione, conversely, if glutathione is not available, the effects of oxidative stress will be more severe (Whitfield 2001).

Processes, like protein phosphorylation, activation of several transcriptional factors, apoptosis, immunity, and differentiation, rely on proper ROS production inside cells. Strategies to counteract the effects of free radicals and oxidative stress, such as superoxide dismutase, affect several cellular structures, such as membranes, lipids, proteins, lipoproteins, and deoxyribonucleic acid (Hermes-Lima and Storey 2004; Pizzino et al. 2017). Interestingly, no effect was observed in lactate dehydrogenase, which has been proposed as a non-specific biomarker of tissue turnover rate, which is a normal metabolic process. Many cancers cause a general increase in lactate dehydrogenase levels or an increase in one of its isozymes. The growth of tumor cells consumes more oxygen than the supply,thus, hypoxia is quite common. Growing tumors undergo lactate dehydrogenase mediated energy production to fulfill the demand for fast cellular growth (Farhana and Lappin 2022).

In general, hematoxylin–eosin histopathological analysis revealed slightly attributable damage in both renal and liver samples. Compared to the control group, all tissues samples in 3 mg/kg of body weight dosage provoked discreet congestion and vascular dilation. Also, frank nuclei with intense coloration indicate nuclear-enhanced activity. Slight congestion is observed at 6 mg/kg, and granular cytoplasm can be appreciated. Central round nucleus with dispersed chromatin and the presence of visible nucleoli can also indicate augmented cell activity. However, since the purpose of the study is to provide a therapeutical window for NCTD, the lack of frank deterioration in procured tissue micrographs was expected.

Pixels are the single minor component of picture elements, and their intensities range between black and white. The magnitude of brightness values in an image is defined as -bit- and specifies image depth and the level of precision in which pixel intensities are coded. ImageJ converts 32-bit images, which can display 2^{32} Gy levels, to 8-bit images that can only display 2^{8}, by linearly scaling from a minimum of 0 to a maximum of 255 Gy levels. This transformation allows to set upper and lower threshold values, to segment grayscale images into micrographs features of interest and background. Nuclei segmentation was achieved by using max-entropy threshold algorithm that maximizes inter-class entropy, which is very useful to segment images with few bright objects on large dark background. Otsu thresholding minimize inter-class variance and divides the image histogram in two classes, foreground, and background, which was used to measure centrilobular and portal triad vein light in liver samples, and convoluted tubules and corpuscles.

Nuclei analysis revealed significant changes in hepatocytes at 3 mg/kg dose group, in *average size* (which talks about cell differentiation), and total size, that could be translated to an augmented nuclear activity. Interestingly, only the 6 mg/kg provoked a significant difference in portal veins *count*, and centrilobular veins and adjacent capillarity *count* and *total area*, parameters that has been used as a hepatic damage biomarker after hepatic resections in small animal models (Xie et al. 2016). Furthermore, both doses' groups provoked an augmentation of *convoluted tubules* average size which incite us to relate it with an augmented elimination rate by kidney clearance.

Conclusion

These physiological effects of NCTD can be exploited as treatment strategies if able to operate in an established posology and proper testing. Nevertheless, we recommend establishing a therapeutical window between the calculated LD_1 and LD_{10} and weighing the beneficial effects against the toxicological effects of this potent molecule. In small animals' models and

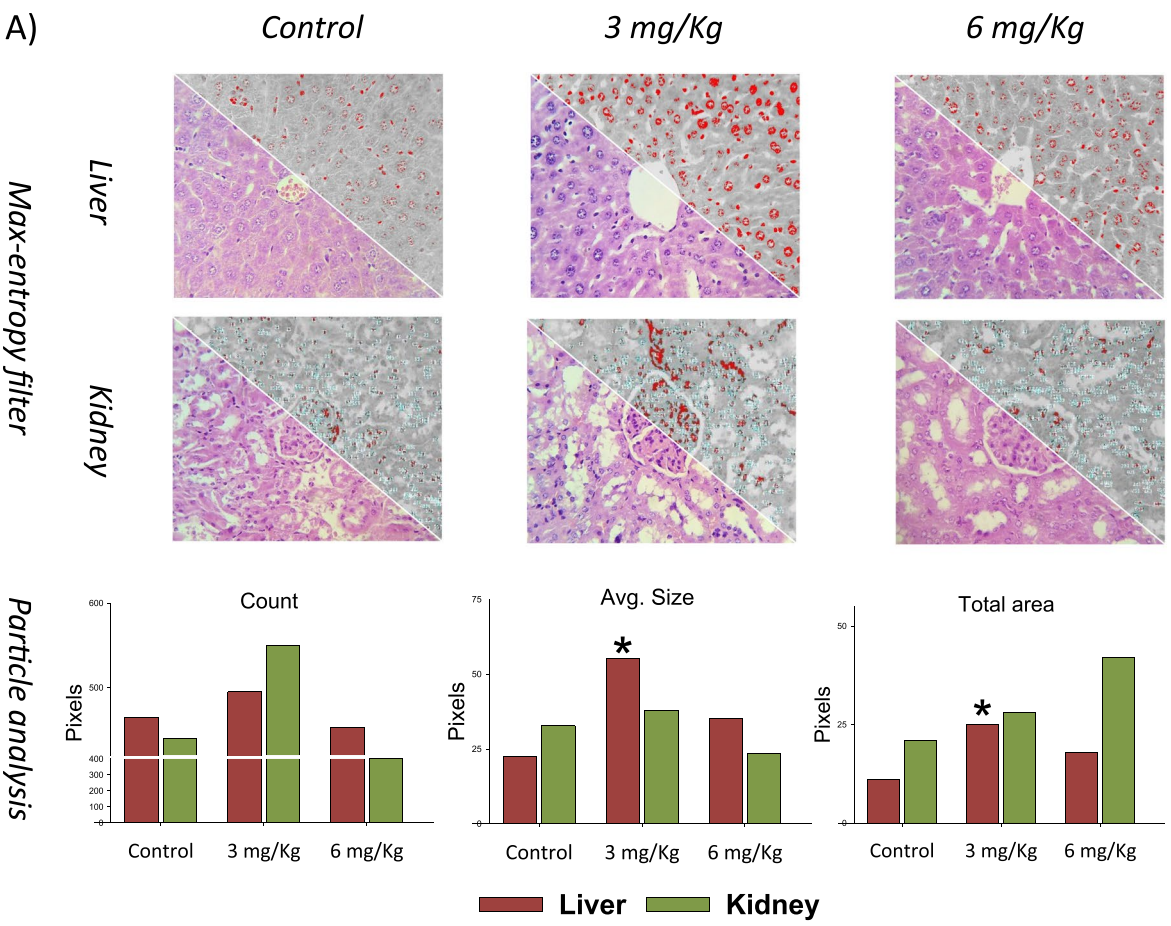
A)
Control
3 mg/Kg
6 mg/Kg
Max-entropy filter
Liver
Kidney
Particle analysis
Count
Avg. Size
Total area
Pixels
Control
3 mg/Kg
6 mg/Kg
Liver
Kidney

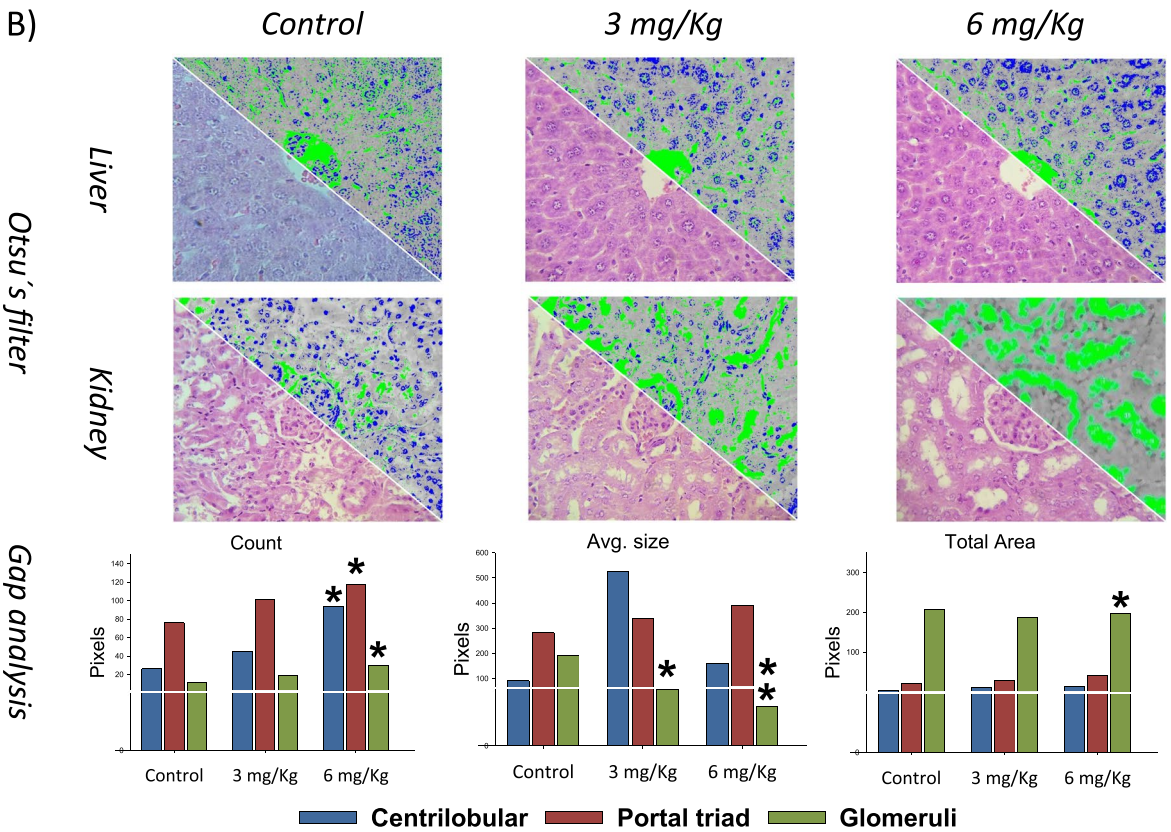
B)
Control
3 mg/Kg
6 mg/Kg
Otsu´s filter
Liver
Kidney
Gap analysis
Count
Avg. size
Total Area
Pixels
Control
3 mg/Kg
6 mg/Kg
Centrilobular
Portal triad
Glomeruli

◂**Fig. 4** Hematoxylin and eosin micrographs multispectral object- and spatial-level quantitative analysis. **A** Contrasted nuclei by max entropy threshold and particle analysis. **B** Vein and adjacent sinusoidal capillaries analysis by Otsu´threshold. Pixel area analysis of multispectral data showed as pixel means ± standard deviation. * $p \leq 0.05$; ** $p \leq 0.01$ significant different compared to the control group

trials context, liver function tests are recommended to monitor liver damage, and if employed as chemotherapeutic agent to include lactate dehydrogenase to assess the type, location, and severity of tissue damage. To our knowledge, there is limited information regarding NCTD effect in a non-pathological scenario which would allow us to objectively evaluate its toxicity and establish an antecedent for future studies in the myriad applications for NCTD in a different pathological context.

Supplementary Information The online version contains supplementary material available at https://doi.org/10.1007/s00210-022-02299-z.

Author contribution GMR conceived, conducted experiments and wrote the manuscript. MLDM, ERM, ECV data curation, formal analysis. JMDLR, DAFB software, validation; visualization. AVL conceived, funding acquisition, project administration, writing—review and editing. All authors read and approved the manuscript and all data were generated in-house and no paper mill was used.

Funding This study was supported by Instituto Politécnico Nacional SIP code 20210197, and 20220561. Author Martínez-Razo G. is a DSc. student who received scholarship from CONACyT and BEIFI-IPN. M.L. Dominguez-López, E. Reyes-Maldonado, José M. de la Rosa, Diego A. Fabila-Bustos and A. Vega-López, are fellows of *Estímulos al Desempeño en Investigación and Comisión y Fomento de Actividades Académicas* (*Instituto Politécnico Nacional*) and *Sistema Nacional de Investigadores* (SNI, CONACyT, México).

Data availability Raw data has been made available.

Declarations

Ethics approval The study protocol was approved by the local Ethical Committee (license number: PE/001/2574–6/20). Healthy BDF1 mice were obtained from the National School of Biological Sciences, Mexico, and were maintained in agreement with Article 38 and Chapter V of the Directive 2010/63/EU of the European Parliament and of the Council of 22 September 2010 on the protection of animals used for scientific purposes.

Consent to participate Not applicable.

Consent for publication Not applicable.

Competing interests The authors declare no competing interests.

References

Ben Salem C, Fathallah N, Hmouda H, Bouraoui K (2011) Drug-induced hypoglycaemia: an update. Drug Saf 34(1):21–45. https://doi.org/10.2165/11538290-000000000-00000

Bjornsson TD (1979) Use of serum creatinine concentrations to determine renal function. Clin Pharmacokinet 4(3):200–222. https://doi.org/10.2165/00003088-197904030-00003

Dorn DC, Kou CA, Png KJ, Moore MA (2009) The effect of cantharidins on leukemic stem cells. Int J Cancer. https://doi.org/10.1002/ijc.24157

Dzul-Caamal R, Hernández-López A, Gonzalez-Jáuregui M, Padilla SE, Girón-Pérez MI, Vega-López A (2016) Usefulness of oxidative stress biomarkers evaluated in the snout scraping, serum and Peripheral Blood Cells of Crocodylus moreletii from Southeast Campeche for assessment of the toxic impact of PAHs, metals and total phenols. Comp Biochem Physiol A Mol Integr Physiol 200:35–46. https://doi.org/10.1016/j.cbpa.2016.05.006

Farhana A, Lappin SL (2022) Biochemistry, lactate dehydrogenase. In: StatPearls [Internet], StatPearls Publishing, Treasure Island. Available from: https://www.ncbi.nlm.nih.gov/books/NBK557536/. Accessed 8 May 2022

Friedman SB, Grota LJ, Glasgow LA (1972) Differential susceptibility of male and female mice encephalomyocarditis virus: effects of castration, adrenalectonomy, and the administration of sex hormones. Infection and Inmmunity 5(5):637–644

Hammer Ø, Harper DAT, Ryan PD (2001) PAST: Paleontological Statistics Software Package for Education and Data Analysis. Palaeontol Electron 4:9. http://palaeo-electronica.org/2001_1/past/issue1_01.htm

Harrisberg J, Deseta JC, Cohen L, Temlett J, Milne FJ (1984) Cantharidin poisoning with neurological complications. S Afr Med J 65(15):614–615

Hermes-Lima M (2004) Oxygen in biology and biochemistry: role of free radicals. In: Storey KB (ed) Functional metabolism: regulation and adaptation. Wiley-Liss Inc., Hoboken, pp 319–351

Honkanen RE (1993) Cantharidin, another natural toxin that inhibits the activity of serine/threonine protein phosphatases types 1 and 2A. FEBS Lett 330(3):283–286. https://doi.org/10.1016/0014-5793(93)80889-3

Legland D, Arganda-Carreras I, Andrey P (2016) MorphoLibJ: integrated library and plugins for mathematical morphology with ImageJ. Bioinformatics 32(22):3532–3534. https://doi.org/10.1093/bioinformatics/btw413

Li YM, Casida JE (1992) Cantharidin-binding protein: identification as protein phosphatase 2A. Proc Natl Acad Sci U S A 89(24):11867–11870. https://doi.org/10.1073/pnas.89.24.11867

Linck B, Boknik P, Knapp J, Müller FU, Neumann J, Schmitz W, Vahlensieck U (1996) Effects of cantharidin on force of contraction and phosphatase activity in nonfailing and failing human hearts. Br J Pharmacol 119(3):545–550. https://doi.org/10.1111/j.1476-5381.1996.tb15706.x

Lu K, Cao M, Mao W, Sun X, Tang J, Shen Y, Sui M (2012) Targeted acid-labile conjugates of norcantharidin for cancer therapy. J Mater Chem 22:15804. https://doi.org/10.1039/c2jm33069e

Madera-Sandoval RL, Tóvári J, Lövey J, Ranđelović I, Jiménez-Orozco A, Hernández-Chávez VG, Reyes-Maldonado E, Vega-López A (2019) Combination of pentoxifylline and α-galactosylceramide with radiotherapy promotes necro-apoptosis and leukocyte infiltration and reduces the mitosis rate in murine melanoma. Acta Histochem 121(6):680–689. https://doi.org/10.1016/j.acthis.2019.06.003

Mei L, Sang W, Cui K, Zhang Y, Chen F, Li X (2019) Norcantharidin inhibits proliferation and promotes apoptosis via c-Met/Akt/mTOR pathway in human osteosarcoma cells. Cancer Sci 110(2):582–595. https://doi.org/10.1111/cas.13900

Min HK, Kapoor A, Fuchs M, Mirshahi F, Zhou H, Maher J, Kellum J, Warnick R, Contos MJ, Sanyal AJ (2012) Increased hepatic synthesis and dysregulation of cholesterol metabolism is associated with the severity of nonalcoholic fatty liver disease. Cell Metab 15(5):665–674. https://doi.org/10.1016/j.cmet.2012.04.004

Misra HP, Fridovich I (1972) The role of superoxide anion in the autoxidation of epinephrine and a simple assay for superoxide dismutase. J Biol Chem 247(10):3170–3175

Moed L, Shwayder TA, Chang MW (2001) Cantharidin revisited: a blistering defense of an ancient medicine. Arch Dermatol. https://doi.org/10.1001/archderm.137.10.1357

Nájera-Martínez M, Landon-Hernández GG, Romero-López JP, Domínguez-López ML, Vega-López A (2022) (2022) Disruption of neurotransmission, membrane potential, and mitochondrial calcium in the brain and spinal cord of Nile tilapia elicited by Microcystis aeruginosa extract: an uncommon consequence of the eutrophication process. Water Air Soil Pollut. 233(1):6. https://doi.org/10.1007/s11270-021-05480-x

Neumann J, Herzig S, Boknik P, Apel M, Kaspareit G, Schmitz W, Scholz H, Tepel M, Zimmermann N (1995) On the cardiac contractile, biochemical and electrophysiological effects of cantharidin, a phosphatase inhibitor. J Pharmacol Exp Ther 274(1):530–539

Pachuta-Stec A, Szuster-Ciesielska A (2015) New Norcantharidin analogs: synthesis and anticancer activity. Arch Pharm (Weinheim) 348(12):897–907. https://doi.org/10.1002/ardp.201500255

Pan MS, Cao J, Yue-Zu F (2020) Insight into norcantharidin, a small molecule synthetic compound with potential multi-target anticancer activities. Chin Med 15:55. https://doi.org/10.1186/s13020-020-00338-6

Pizzino G, Irrera N, Cucinotta M, Pallio G, Mannino F, Arcoraci V, Squadrito F, Altavilla D, Bitto A (2017) Oxidative stress: harms and benefits for human health. Oxid Med Cell Longev 2017:8416763. https://doi.org/10.1155/2017/8416763

R Core Team (2022) R: a language and environment for statistical computing. R Foundation for Statistical Computing, Vienna. https://www.R-project.org/. Accessed 4 Jul 2022

Schneider CA, Rasband WS, Eliceiri KW (2012) NIH Image to ImageJ: 25 years of image analysis. Nat Methods 9(7):671–675. https://doi.org/10.1038/nmeth.2089

Tinklenberg RL, Murphy SD, Mochel JP, Seo YJ, Mahaffey AL, Yan Y, Ward JL (2020) Evaluation of dose-response effects of short-term oral prednisone administration on clinicopathologic and hemodynamic variables in healthy dogs. Am J Vet Res 81(4):317–325. https://doi.org/10.2460/ajvr.81.4.317

Vroon DH, Israili Z (1990) Aminotransferases. In: Walker HK, Hall WD, Hurst JW (eds) Clinical methods: the history, physical, and laboratory examinations, 3rd edn. Butterworths, Boston (99:492-493)

Whitfield JB (2001) Gamma glutamyl transferase. Crit Rev Clin Lab Sci 38(4):263–355. https://doi.org/10.1080/20014091084227

Xie C, Schwen LO, Wei W, Schenk A, Zafarnia S, Gremse F, Dahmen U (2016) Quantification of hepatic vascular and parenchymal regeneration in mice. PLoS ONE 11(8):e0160581. https://doi.org/10.1371/journal.pone.0160581

Xie MH, Ge M, Peng JB, Jiang XR, Wang DS, Ji LQ, Ying Y, Wang Z (2019) In-vivo anti-tumor activity of a novel poloxamer-based thermosensitive in situ gel for sustained delivery of norcantharidin. Pharm Dev Technol 24(5):623–629. https://doi.org/10.1080/10837450.2018.1550788

Zhang Y, Klaassen CD (2013) Hormonal REgulation of Cyp4a Isoforms in mouse liver and kidney. Xenobiotica 43(12):1055–1063. https://doi.org/10.3109/00498254.2013.797622

Zhou J, Ren Y, Tan L, Song X, Wang M, Li Y, Cao Z, Guo C (2020) Norcantharidin: research advances in pharmaceutical activities and derivatives in recent years. Biomed Pharmacother 131:110755. https://doi.org/10.1016/j.biopha.2020.110755